 doi:10.20944/preprints202210.0311.v1

Article

Periodontal tissue regeneration by recombinant human collagen peptide granules applied with β-tricalcium phosphate fine particles

Yuto Yoshino[1], Hirofumi Miyaji[1,*], Erika Nishida[1], Yukimi Kanemoto[1], Asako Hamamoto[1], Akihito Kato[1], Tsutomu Sugaya[1], Tsukasa Akasaka[2]

[1] Department of Periodontology and Endodontology, Faculty of Dental Medicine, Hokkaido University; yutoy0526@den.hokudai.ac.jp (Y.Y.); miyaji@den.hokudai.ac.jp (H.M.); erikanishida@den.hokudai.ac.jp (E.N.); yukimikanemoto@den.hokudai.ac.jp (Y.K.); ymmha7@gmail.com (A.H.); akito@den.hokudai.ac.jp (A.K.); sugaya@den.hokudai.ac.jp (T.S.)

[2] Department of Periodontology and Endodontology, Faculty of Dental Medicine, Hokkaido University; akasaka@den.hokudai.ac.jp

* Correspondence: miyaji@den.hokudai.ac.jp (H.M.); Tel.: +81-11-706-4266 (H.M.)

Abstract: Recombinant human collagen peptide (RCP) is a recombinantly created xeno-free biomaterial enriched in RGD (arginine-glycine-aspartic acid) sequences, with good processability that is being investigated for regenerative medicine applications. Recently, the biocompatibility and osteogenic ability of β-TCP/RCP (RCP granules combined with β-tricalcium phosphate (TCP) submicron particles) were demonstrated. In the present study, β-TCP/RCP was implanted into experimental periodontal tissue defects (three-walled bone defect) created in beagle dogs to investigate tissue responses and subsequent regenerative effects. Micro computed tomography image analysis at 8 weeks postoperatively showed that the amount of new bone after β-TCP/RCP graft was significantly greater (2.2 fold, $P<0.05$) than that of the control (no graft) group. Histological findings showed that the transplanted β-TCP/RCP induced active bone-like tissue formation including TRAP-positive and OCN-positive cells as well as bioabsorbability. Ankylosis did not occur, and periostin-positive periodontal ligament-like tissue formation was observed. Histological measurements revealed that β-TCP/RCP implantation formed 1.7-fold more bone-like tissue and 2.1-fold more periodontal ligament-like tissue than the control, and significantly suppressed gingival recession and epithelial downgrowth ($P<0.05$). These results suggest that β-TCP/RCP is effective as a periodontal tissue regenerative material.

Keywords: Animal study; beagle dog; β-tricalcium phosphate (TCP); immunohistochemistry; micro computed tomography (CT); periodontal tissue engineering; periostin; recombinant human collagen peptide (RCP); scaffold material; 3-wall intrabony defect

1. Introduction

Periodontal regenerative therapy was developed to regenerate periodontal attachments, such as the periodontal ligament, cementum, and alveolar bone, lost due to severe periodontitis. Recently, the concept of tissue engineering has been incorporated into periodontal regenerative therapy [1, 2], whereby cells [3-5], signaling molecules (growth factors) [6, 7], and scaffold materials [8, 9] are jointly used for tissue regeneration. Scaffolds play an important role in promoting cell adhesion, proliferation, differentiation, and subsequent extracellular matrix deposition and blood vessel network establishment in tissue defects [10, 11]. In addition, due to their mechanical properties, scaffolds maintain the regenerative space and store growth and nutritional factors [12].

Various materials have been used as scaffolds for periodontal tissue engineering. In particular, the natural polymer collagen has excellent biocompatibility and bioabsorbability [13]. It has been reported that the implantation of collagen scaffolds in a canine

 doi:10.20944/preprints202210.0311.v1

periodontal defect model promoted reconstruction of periodontal ligament, cementum, and alveolar bone [14, 15]. However, commercially available collagen scaffolds are derived from domestic animal tissues, such as cows and pigs, and have the risk of bio-contamination and antigenicity, and are currently not a completely safe and secure medical material for use in humans [16]. Against this backdrop, recombinant human collagen peptide (RCP), based on the human type I collagen (α1 chain), was recently created to circumvent the problems associated with animal-derived collagen [17].

RCP is recombinantly produced by yeast to lack animal-derived components (xeno-free) and designed with an amino acid sequence that does not contain antigenic moieties. Compared to natural collagen, RCP contains more arginine-glycine-aspartic acid (RGD) sequences, which are important for cell adhesion and differentiation [18]. Like natural collagen, RCP can be processed to many forms by cross-linking and exhibits bioabsorbable properties in the body; therefore, RCP has great potential as a scaffold material in vivo [19, 20]. Several studies have shown that a sponge made from RCP exhibits good properties as a scaffold for bone marrow stromal cells and adipose-derived stem cells [21, 22].

However, collagen-based scaffolds generally suffer from low osteoconductive capacity compared to bioceramic materials [23]. Therefore, a combination of collagen and various bioceramics has been investigated to increase the amount of bone formation. Murakami et al. combined bovine-derived collagen scaffolds with fine (submicron scale) particle β-tricalcium phosphate (β-TCP) [24]. They found biological activities, such as cell proliferation, protein adsorption, and bone tissue formation, of the composite scaffold were increased compared to a collagen scaffold alone. Furthermore, the composite scaffold was effective in periodontal tissue reconstruction in a canine experimental periodontal defect model [25]. Combinations with collagen and other types of bioceramics, such as octacalcium phosphate or low-crystalline hydroxyapatite, also showed excellent bone or periodontal tissue forming effects [26-29].

Based on these studies, Furihata et al. prepared RCP granules with β-TCP fine particles (β-TCP/RCP) and showed a significant promotion of osteoblast growth and differentiation, as well as in vivo (in rat) bone formation, compared to normally granulated RCP (without β-TCP) [30]. Therefore, we hypothesized that β-TCP/RCP represents a promising scaffold material for periodontal tissue engineering. The purpose of this study was to evaluate the effect of β-TCP/RCP on periodontal tissue reconstruction. β-TCP/RCP was implanted into periodontal tissue defects (three-wall intrabony defects) created in the canine mandible, and reconstruction of periodontal tissue was examined by micro computed tomography (micro-CT) image analysis and histological observation.

2. Results

2.1 Evaluation by micro-CT imaging

Figure 1A shows micro-CT images of periodontal tissue defects. At 4 weeks, the β-TCP/RCP group showed slight formation of new bone (radiopaque area) at the bottom of bone defect (indicated by the yellow dashed line). In the Ctrl group, slight formation of new bone was shown in the bone defect, similar to the β-TCP/RCP group. The vertical height of the mesial wall of the bone defect (arrows) in the Ctrl group tended to be lower than in the β-TCP/RCP group. Micro-CT images of the 8-week β-TCP/RCP group showed that most of the bone defect was filled with newly formed bone. Notably, a periodontal ligament-like space (no direct contact between alveolar bone and root) existed between the new bone and the tooth root. The vertical height of the mesial wall of the bone defect was maintained as in the 4-week group. In contrast, although the opaque density increased in the Ctrl group, only slight bone formation was observed in the defect. Moreover, the upper region of the bone defect area showed radiolucency, and the mesial wall of the bone defect was low as in the 4-week group.

Preprints (www.preprints.org) | NOT PEER-REVIEWED | Posted: 20 October 2022 doi:10.20944/preprints202210.0311.v1

Quantitative evaluation of bone volume at 8 weeks postoperatively showed that the mean + standard deviation of new bone volume (×10^4 pixel) was 12.9 + 3.5 and 6.0 + 2.1 in the β-TCP/RCP group and Ctrl group, respectively. The β-TCP/RCP group had approximately 2.2 times more new bone than the Ctrl group, and there was a significant difference between the two groups (P<0.05) (Figure 1B).

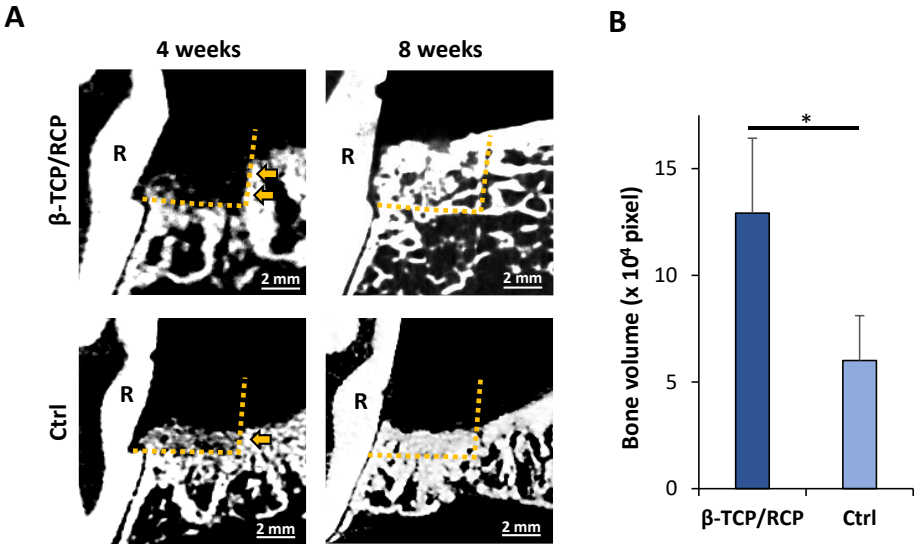

Figure 1. Micro CT analysis. (A) Micro-CT images of a mesial-distal cross section of bone defects. The yellow dashed lines and arrows indicate the border of the bone defect and the mesial bone wall, respectively. (B) Bone volume (n = 3, mean + standard deviation). *: P < 0.05. Statistical analysis: two-tailed Mann-Whitney's U test. Abbreviations: CT, computed tomography; Ctrl, control; R, root; RCP, recombinant human collagen peptide; TCP, tricalcium phosphate. centered.

2.2 Histological observation at 4 weeks

Figure 2 shows masson trichrome (MT)-stained and OCN immuno-stained sections at 4 weeks postoperatively (the left column of Supplemental Figure 1 shows hematoxylin eosin (HE) stained sections at 4 weeks). New bone-like tissue was formed continuously from the pre-existing alveolar bone in the β-TCP/RCP area remaining in the defect (Figure 2A). The defect region containing residual β-TCP/RCP and bone-like tissue was covered by fibrous tissue (FT) derived from the gingiva on the coronal side, and the down-growth of the junctional epithelium was arrested at the cement-enamel junction (Figure 2B, arrow). Cross-sections of the residual β-TCP/RCP showed reticular structures of non-uniform size, and dark blue-stained new bone-like tissue was found in the inner regions of the reticular structures (Figure 2C). Residual β-TCP/RCP granules close to the root or gingiva tended to show less bone-like tissue formation in and around the granules. Although there was no ankylosis between the root surface and the new bone-like tissue, the formation of periodontal ligament-like tissue was not clear due to residual β-TCP/RCP (Figure 2C). OCN immunostaining was performed to confirm the presence of osteoblastic cells around the newly formed bone. OCN-positive cells (dark brown) were observed close to the newly formed bone-like tissue in the reticular structure of the β-TCP/RCP group (Figure 2D). In the Ctrl group at 4 weeks postoperatively, new bone-like tissue was formed in the defect area that was continuous with the pre-existing bone, which has rich bone trabeculae (Figure 2E). The gingival fibrous tissue was close to the root surface and filled most of the defect, while the junctional epithelium grew down along the root surface to

Preprints (www.preprints.org) | NOT PEER-REVIEWED | Posted: 20 October 2022 doi:10.20944/preprints202210.0311.v1

the center of the defect (arrows in Figure 2F), with no periodontal ligament-like tissue formation (Figure 2F).

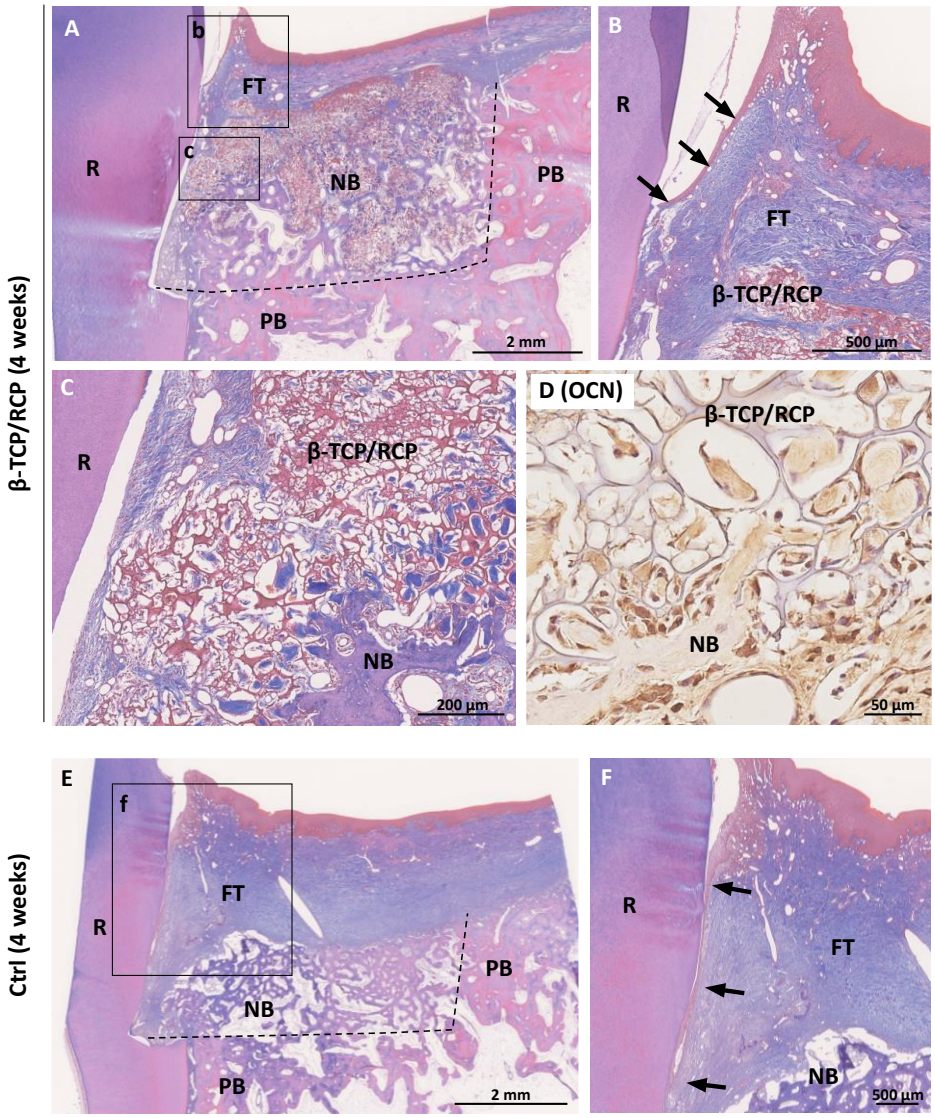

Figure 2. Histological findings at 4 weeks. (A) Histological image of a β-TCP/RCP group specimen. (B) Higher magnification image related to framed area (b) in panel A. Arrows indicate junctional epithelium. (C) Higher magnification image related to framed area (c) in panel A. (D) OCN-positive cells (dark brown) related to β-TCP/RCP and new bone-like tissue. (E) Histological image of a Ctrl group specimen. (F) Higher magnification image related to framed are (f) in panel E. Arrows indicate junctional epithelium. (A-C, E, F) Masson trichrome staining, (D) OCN immunostaining. The black dashed lines indicate the border of the bone defects. Abbreviations: Ctrl, control; FT, fibrous tissue; NB, new bone-like tissue; OCN, osteocalcin; PB, pre-existing bone; R, root; RCP, recombinant human collagen peptide; TCP, tricalcium phosphate.

Figure 3 shows the results of TRAP, CD3, CD204, and POSTIN immunostaining at 4 weeks postoperatively. TRAP staining showed that TRAP-positive osteoclastic cells (red) were frequently observed around the bone-like tissue formed by β-TCP/RCP implantation, especially in the region adjacent to the pre-existing bone, but rarely on the gingival side. In the Ctrl group, the expression of TRAP-positive cells was especially high in the superficial area of the new bone-like tissue. CD3-positive lymphocytes (dark brown) were only found in the gingival fibrous tissue adjacent to the gingival sulcus on the coronal side in both groups (probably due to attack by periodontal pocket flora) and were negative around the implanted β-TCP/RCP. The distribution of CD204-positive macrophages (dark brown) was distinctive; they were detected in association with the β-TCP/RCP residues in the defect, especially in the area close to the gingival fibrous tissue. In addition, strong

Preprints (www.preprints.org) | NOT PEER-REVIEWED | Posted: 20 October 2022 doi:10.20944/preprints202210.0311.v1

positive expression was also observed in residues of β-TCP/RCP close to the root surface. In contrast, CD204 staining was negative in the control group. POSTIN was expressed (dark brown) in the pre-existing periodontal ligament and in the space between the root and the new bone-like tissue. In the coronal region of the defect, POSTIN expression was weak, and was especially negative in the area of epithelial down-growth (arrows) in the control group.

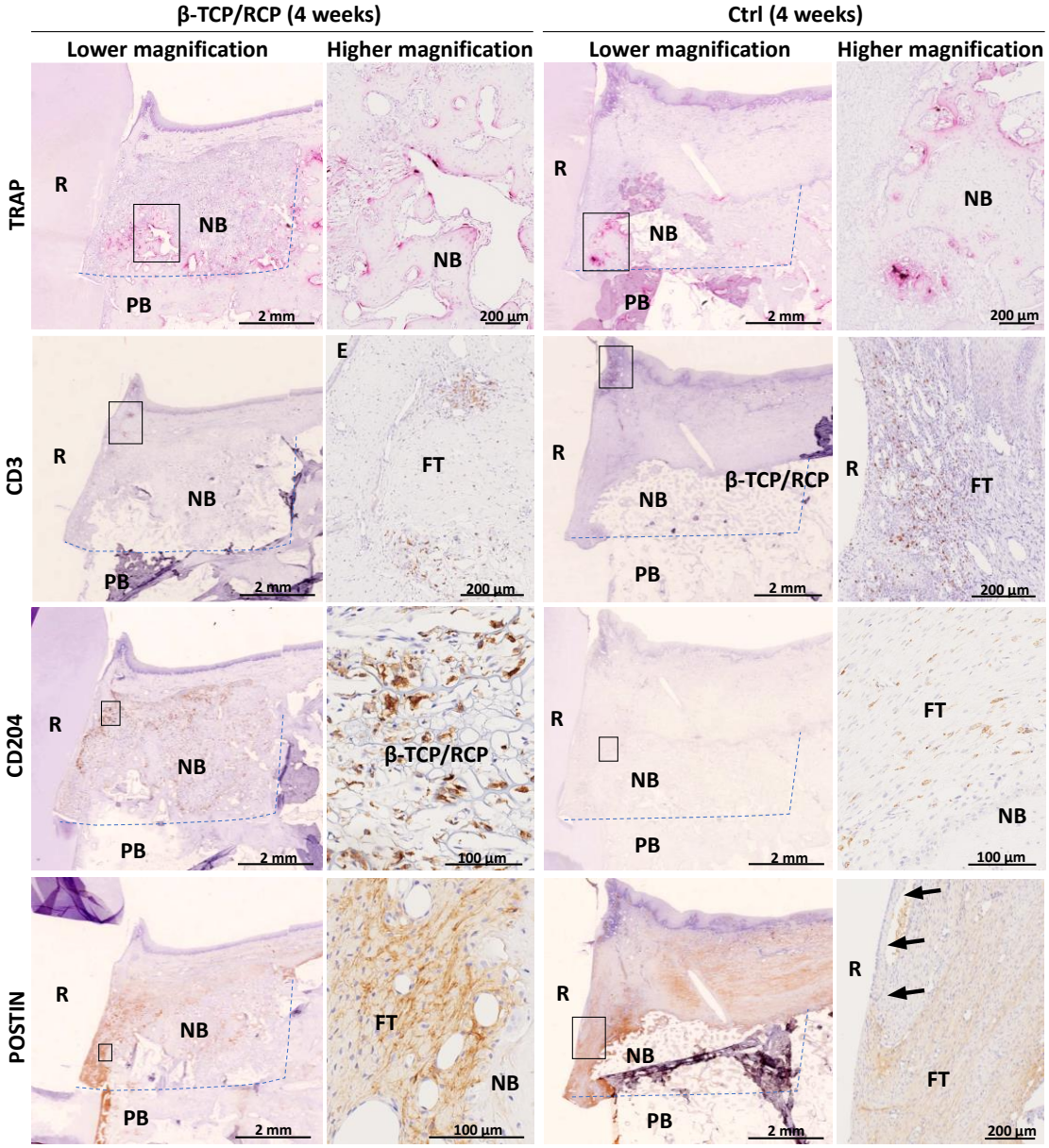

Figure 3. TRAP staining (red) and CD3, CD204 and POSTIN immunostaining (dark brown) at 4 weeks. The high-magnification images in the right column of each group show the framed areas in the adjacent low-magnification image in the left column. Arrows in POSTIN staining of the Ctrl group indicate junctional epithelium. The blue dashed lines indicate the border of the bone defects. Abbreviations: Ctrl, control; FT, fibrous tissue; NB, new bone-like tissue; PB, pre-existing bone; POSTIN, periostin; R, root; RCP, recombinant human collagen peptide; TCP, tricalcium phosphate; TRAP, tartaric acid-resistant acid phosphatase.

Preprints (www.preprints.org) | NOT PEER-REVIEWED | Posted: 20 October 2022 doi:10.20944/preprints202210.0311.v1

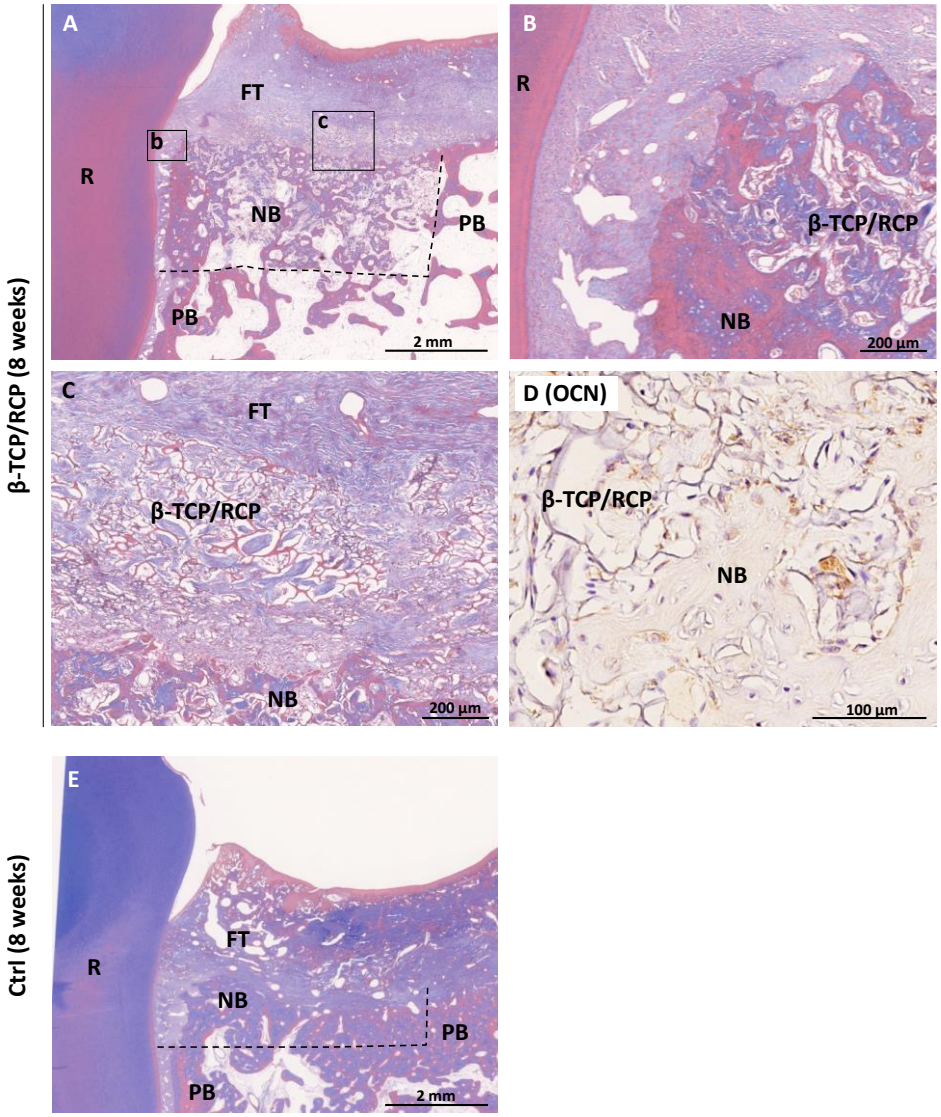

Figure 4. Histological findings at 8 weeks. (A) Histological image of a β-TCP/RCP group specimen. (B) Higher magnification image related to framed area (b) in panel A. (C) Higher magnification image related to framed area (c) in panel A. (D) OCN-positive cells (dark brown) related to β-TCP/RCP and new bone-like tissue. (E) Histological image of a Ctrl group specimen. (A-C, E) Masson trichrome staining, (D) OCN immunostaining. The black dashed lines indicate the border of the bone defects. Abbreviations: Ctrl, control; FT, fibrous tissue; NB, new bone-like tissue; OCN, osteocalcin; PB, pre-existing bone; R, root; RCP, recombinant human collagen peptide; TCP, tricalcium phosphate.

2.3 Histological observation at 8 weeks

Figure 4 shows MT-stained and OCN-immunostained sections at 8 weeks postoperatively (the right panel in Supplementary Figure 1 shows HE-stained sections at 8 weeks). In the β-TCP/RCP group, β-TCP/RCP remained in the defect as observed at 4 weeks; however, its shape and internal structure were unclear, and much bone-like tissue was observed within the β-TCP/RCP implantation region. Down-growth of the junctional epithelium stopped around the tooth cervical region (Figure 4A). Periodontal ligament-like tissue was found in the space between the root and the new bone-like tissue, and was continuous with the pre-existing periodontal ligament. No ankylosis was observed in this study (Figure 4B). Residual β-TCP/RCP was also scattered within the gingival fibrous tissue, and no bone-like tissue formation was observed in the surrounding areas, with fibrous tissue invading the granules (Figure 4C). OCN immunostaining indicated that OCN-positive cells were present around the bone-like tissue found around the β-TCP/RCP, as observed at 4 weeks (Figure 4D). At 8 weeks, the Ctrl group showed new bone-like tissue that was continuous with the pre-existing bone in the defect, and thicker and denser bone trabeculae compared to 4 weeks (Figure 4E).

Preprints (www.preprints.org) | NOT PEER-REVIEWED | Posted: 20 October 2022 doi:10.20944/preprints202210.0311.v1

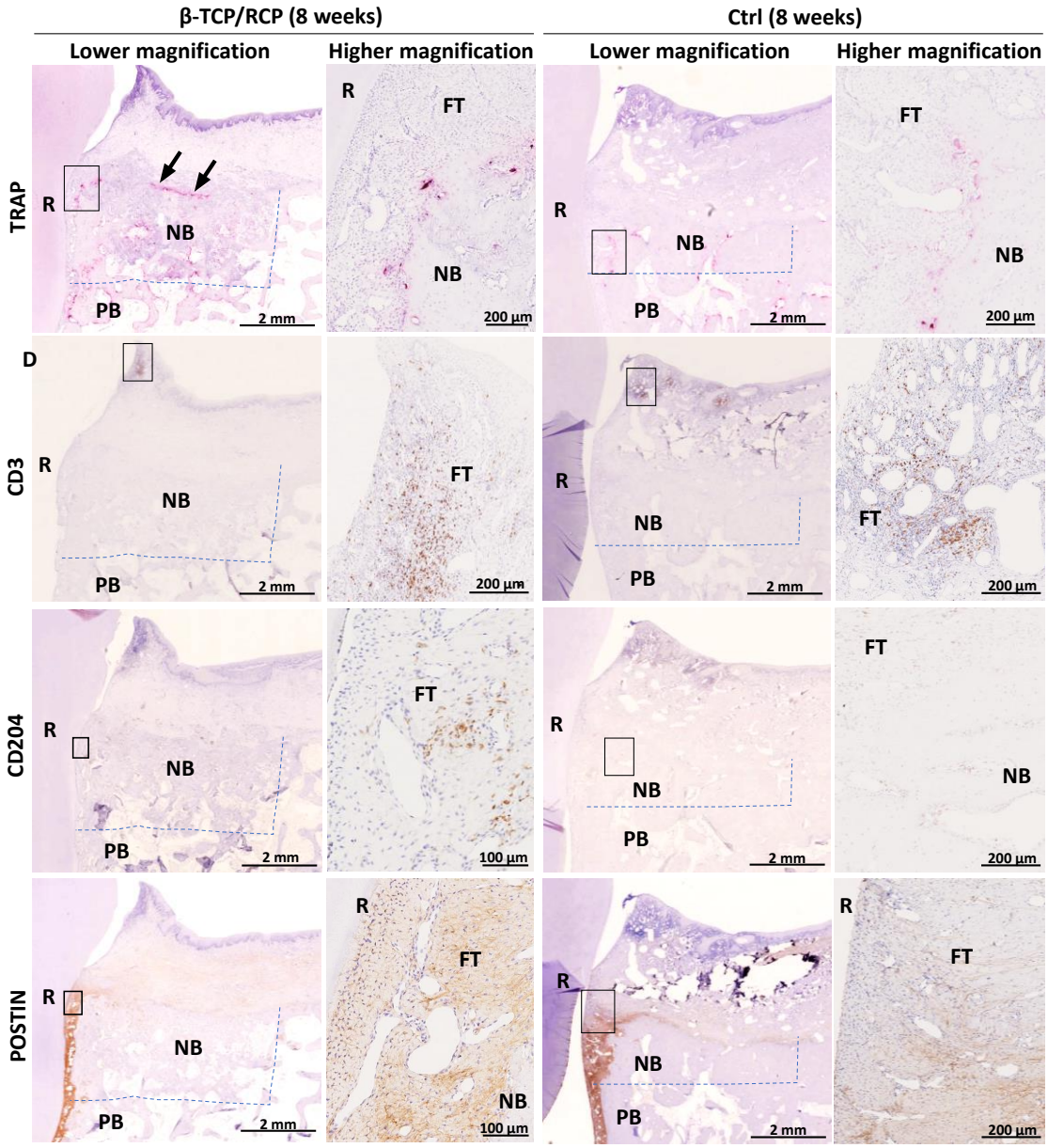

Figure 5. TRAP staining (red) and CD3, CD204 and POSTIN immunostaining (dark brown) at 8 weeks. The high-magnification image in the right column of each group shows the framed area in the adjacent low-magnification image in the left column. Arrows in TRAP staining of the β-TCP/RCP group indicate that TRAP-positive cells were close to gingival fibrous tissue. The blue dashed lines indicate the border of the bone defects. Abbreviations: Ctrl, control; FT, fibrous tissue; NB, new bone-like tissue; PB, pre-existing bone; POSTIN, periostin; R, root; RCP, recombinant human collagen peptide; TCP, tricalcium phosphate; TRAP, tartaric acid-resistant acid phosphatase.

Figure 5 shows the results of TRAP, CD3, CD204, and POSTIN immunostaining at 8 weeks postoperatively. In contrast to 4 weeks postoperatively, TRAP-positive cells in the β-TCP/RCP group were dispersed throughout the bone defect and were particularly strongly observed at the borders between the bone-like tissue and gingival fibrous tissue (arrows) or periodontal ligament-like tissue. In the control group, TRAP-positive cells were also found in the bone-like tissue located close to the periodontal ligament-like tissue. CD3-positive cells were located within the fibrous tissue of the free gingiva in both groups as at 4 weeks and were not observed around the residual β-TCP/RCP. CD204-positive cells were found around the residual β-TCP/RCP; however CD204 expression tended to be lower compared to that at 4 weeks. CD204 staining was negative in the control group. POSTIN staining revealed expression between the root and the new bone-like

Preprints (www.preprints.org) | NOT PEER-REVIEWED | Posted: 20 October 2022 doi:10.20944/preprints202210.0311.v1

tissue that continued to the preexisting periodontal ligament in both groups. Some fiber bundle structures were observed between the root surface and the new bone-like tissue.

2.4 Histological measurements

Histological measurements of the stained images at 8 weeks revealed that in the β-TCP/RCP and Ctrl groups, gingival tissue height was 4.9+0.7 mm and 3.1+0.7 mm, junctional epithelium height was 3.7+0.2 mm and 2.7+0.5 mm, new bone height was 2.2+0.2 mm and 1.3+0.2 mm, and POSTIN expression tissue height was 2.8+1.0 mm and 1.4+0.2 mm, respectively. These values for the β-TCP/RCP group were approximately 1.6-, 1.3-, 1.7-, and 2.1-fold higher than the Ctrl group, respectively, and significant differences were detected between the two groups for all parameters ($P<0.05$) (Figure 6).

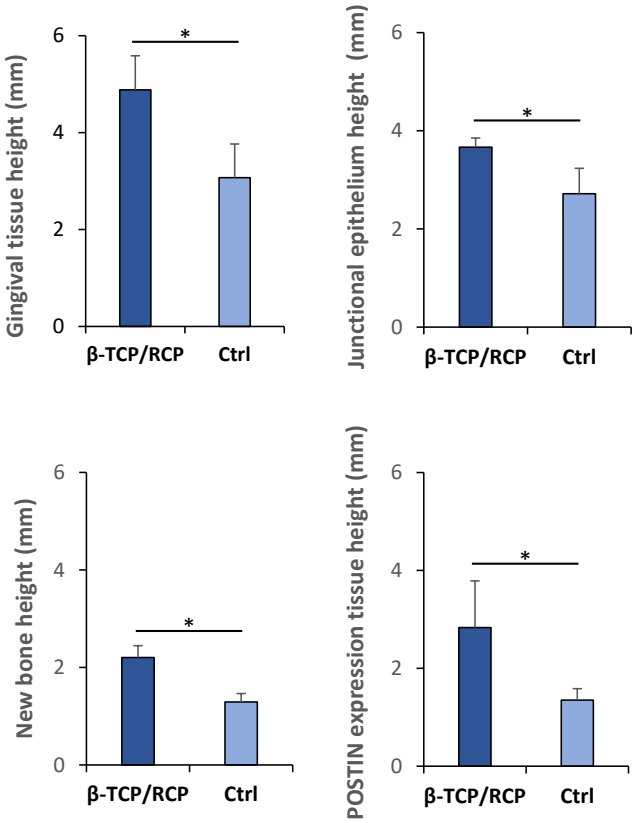

Figure 6. Results of histometric measurements. The height of gingival tissue, junctional epithelium, new bone and POSTIN expression tissue (n = 3, mean + standard deviation). *: $P < 0.05$. Statistical analysis: two-tailed Mann-Whitney's U test. Abbreviations: Ctrl, control; POSTIN, periostin; RCP, recombinant human collagen peptide; TCP, tricalcium phosphate.

3. Discussion

Quantitative analysis using micro-CT images at 8 weeks postoperatively showed that the β-TCP/RCP group had a significantly greater amount of new bone (radiopaque area) than the Ctrl group (Figure 1A and 1B). The radiopaque areas were generally consistent with the MT-stained new bone-like tissue areas (Figure 2 and 4) and the large number of OCN-positive osteoblast-like cells. Furthermore, histological measurements showed that the β-TCP/RCP group had significantly greater new bone height than the Ctrl group (Figure 6). These results suggest that β-TCP/RCP implantation promoted bone healing. Furihata et al. reported that co-culture of β-TCP/RCP and osteoblast-like cells promoted mRNA expression of the osteogenic markers runt-related transcription factor 2 (Runx2), alkaline phosphatase, and bone sialoprotein, to simultaneously stimulate integrin β1 expression [30]. Integrin-mediated cell adhesion to extracellular matrix components, such as type I collagen, is known to activate focal adhesion kinase and its downstream target, bone morphogenetic protein (BMP)-smad signaling, which is involved in promoting osteoblast

 doi:10.20944/preprints202210.0311.v1

differentiation [31]. Verstappen et al. reported that the adhesion of osteoblasts to RGD-modified material via integrins promoted the proliferation and differentiation of osteoblasts, and that the expression of osteogenic markers, such as Runx2 and osteopontin (OPN), was higher compared to those without RGD modification [32]. Since genetic engineering was used to design β-TCP/RCP to contain many RGD sequences [17, 18], it is expected that integrin-mediated cell adhesion frequently occurs in vivo, thereby promoting osteoblast differentiation and bone formation at the β-TCP/RCP implantation site. In addition, β-TCP/RCP is supplemented with sub-micron β-TCP. Calcium and phosphate ions released from β-TCP reportedly play a major role in bone formation [32, 33]. Chang et al. demonstrated that increases in calcium ion and phosphate concentrations promote bone cell mineralization [34]. Dvorak et al. reported that increasing extracellular calcium concentrations promoted osteoblast proliferation and increased expression of the bone formation markers OCN and OPN [35]. Kanatani et al. showed that increasing inorganic phosphate concentrations inhibited osteoclast differentiation and bone resorption activity [36]. It was a distinctive finding that TRAP-positive cells were localized at the base of the bone defect at week 4, whereas high expression was detected throughout the whole defect at week 8 (Figures 3 and 5). Hence, it seems likely that the large amount of calcium and phosphate ions released from the β-TCP submicron particles in the early stage of osteogenesis caused early bone tissue deposition and suppression of osteoclasts to consequently promote bone formation. In previous studies, it has been shown that the combination of β-TCP submicron particles with a collagen sponge induced protein adsorption, and cell adhesion and proliferation [24, 25], which is considered to be due to the increase in material surface area. These findings suggest that the addition of β-TCP submicron particles may have further augmented the biological potential of RCP.

In periodontal regenerative therapy, it is generally considered beneficial to inhibit downgrowth of the junctional epithelium, thereby maintaining the regenerative space until bone is formed [37]. Micro CT images at 4 weeks after surgery showed radiolucency (presumably no bone formation) in the coronal region of the defects in both the β-TCP/RCP and Ctrl groups (Fig. 1A). However, based on the evidence described below, we speculate that the β-TCP/RCP implantation prevents epithelial downgrowth and maintains the regenerative space, although bone regeneration after 4 weeks is still insufficient. (i) Histological observations at 4 weeks showed that the grafted β-TCP/RCP (not visible on X-ray) filled the defect in the β-TCP/RCP group, whereas gingival fibrous tissue filled most of the defect in the Ctrl group (Figures 2A and 2E). (ii) The Ctrl group showed epithelial downgrowth to the middle of the defect (Figures 2F) and failed to maintain the height of the mesial wall of the surgically created bone defect (Figure 1A and 2E). (iii) Histological measurements showed significantly higher junctional epithelial height in the β-TCP/RCP group compared to the Ctrl group (Figure 6). On the other hand, RCP promotes proliferation of several types of cells, such as mesenchymal stromal cells, as reported by Muraya et al. [38], and synovial mesenchymal cells, as reported by Naritomi et al. [39]. In the present study, β-TCP/RCP was found in the gingival fibrous tissue 8 weeks after implantation (Figure 4C), however, these β-TCP/RCP granules were not related to osteogenesis. The ability of β-TCP/RCP to induce mesenchymal cells was limited in gingival fibrous tissue. For example, in severe periodontitis with large bone lesions, β-TCP/RCP is presumably less prone to ectopic bone formation beyond the region surrounded by bone walls. In recent years, attempts have been made to promote bone regeneration using scaffolds in combination with undifferentiated mesenchymal stem cell transplantation and growth factors [40, 41]. Thus, β-TCP/RCP should be included in these methods in the future to increase the amount of bone regeneration.

The periodontal ligament connects the cementum to the alveolar bone in normal periodontal tissue. Since the periodontal ligament is an important structure involved in mastication, it should be regenerated at the same time as alveolar bone formation in periodontal tissue regeneration therapy [42]. When biomaterials that strongly regenerate bone are implanted, adhesion between the new bone and the root of the tooth (ankylosis) may be observed without formation of the periodontal ligament. For example, ankylosis

 doi:10.20944/preprints202210.0311.v1

reportedly occurred as a result of implantation of a BMP-loaded scaffold in a cat root furcation with simultaneous induction of bone regeneration [43]. In the present study, no ankylosis was observed and POSTIN-positive fibrous tissue along the root was shown in the β-TCP/RCP group (Figures 3 and 5). POSTIN is a secreted matricellular protein that is commonly expressed in the periodontal ligament or periosteum [44, 45] and is a marker for periodontal ligament regeneration [46-48]. Therefore, POSTIN-positive regions in the β-TCP/RCP group may represent the periodontal ligament or its precursor tissue, suggesting regeneration of the periodontal ligament following β-TCP/RCP grafting. Cementum regeneration, which serves as an anchor for fiber bundles, is important for periodontal ligament regeneration [49]; unfortunately, no obvious cementum formation was identified in the present study. However, β-TCP/RCP remained in the regeneration site at 8 weeks after implantation, suggesting that further remodeling may subsequently occur to reconstruct the periodontal apparatus.

The implantation site of periodontal tissue regenerative materials is constantly exposed to the risk of infection by oral bacteria because of its location close to the oral cavity [50]. Therefore, rapid resorption and tissue replacement of grafted material are required. Ogawa et al. implanted a bovine collagen sponge containing β-TCP, which was created based on the same concept as the present study, into a canine bone defect and confirmed that it was completely resorbed in 4 weeks [25]. In this study, the mesh structure of residual β-TCP/RCP gradually became sparse by 8 weeks, and CD204-positive M2 macrophage expression was observed around β-TCP/RCP granules, suggesting that the residual β-TCP/RCP was undergoing degradation and resorption. Accordingly, the replacement of β-TCP/RCP appears to be slower than that of the beta-TCP-blended bovine collagen scaffold previously reported by Ogawa et al. [25]. The slow resorption of β-TCP/RCP was likely caused by the non-connected pore structure (calf-derived collagen sponge has a fully connected pore structure) and a difference in the degree of cross-linking [30]. However, there was almost no accumulation of CD3-positive cells to β-TCP/RCP, suggesting that there is no concern about detrimental inflammatory reactions against periodontal tissue regeneration caused by residual β-TCP/RCP [51]. The RCP comprising β-TCP/RCP was designed to exclude the antigenic sites of natural collagen, which accounts for its low inflammatory potential. In addition, bioceramics such as β-TCP are non-absorbable, or must remain in vivo for more than a half year to be absorbed and can inhibit tissue replacement [52, 53]. In this project, β-TCP was added to promote bone formation through ion supply, but was adjusted to a submicron size to ensure smooth resorption. As a result, no residual β-TCP was observed histologically, which is consistent with previous reports [30] and suggests that it does not produce long-term effects on tissue replacement and periodontal regeneration.

4. Materials and Methods

4.1 Fabrication of β-TCP/RCP

β-TCP/RCP was fabricated according to the method of Furihata et al. [30]. An RCP solution (7.5%, Cellnest; Fujifilm Wako Pure Chemical Corp., Osaka, Japan) was lyophilized and granulated using a granulator (Quadroco Mill U5; Quadro Engineering, Waterloo, Canada) into particles approximately 1 mm in diameter. RCP granules were then thermally cross-linked at 142°C for 5 hours and dried using a vacuum drying oven (DP-43; Yamato Scientific Co., Ltd., Tokyo, Japan). The size of RCP granules was measured as the median diameter (D50) by an automated particle size analyzer (Morphologi G3; Malvern Panalytical Ltd., Malvern, UK), to confirm the average diameter to be approximately 1 mm.

Next, β-TCP (β-TCP-100 milled product; Taihei Chemical Industrial Co., Ltd., Osaka, Japan) was dispersed in water using a wet pulverization/dispersion device (Nanovator NVL-AS200-D10; Yoshida Kikai Co., Ltd., Nagoya, Japan). The particle size distribution of β-TCP was measured using a laser diffraction particle size analyzer (SALD-2100; Shimadzu Corporation, Kyoto, Japan), to confirm an average diameter of 0.73 μm.

Preprints (www.preprints.org) | NOT PEER-REVIEWED | Posted: 20 October 2022 doi:10.20944/preprints202210.0311.v1

Subsequently, 500 μL of β-TCP dispersion (1 wt%) was added to 100 mg of RCP granules to swell and form β-TCP/RCP (Figure 7A).

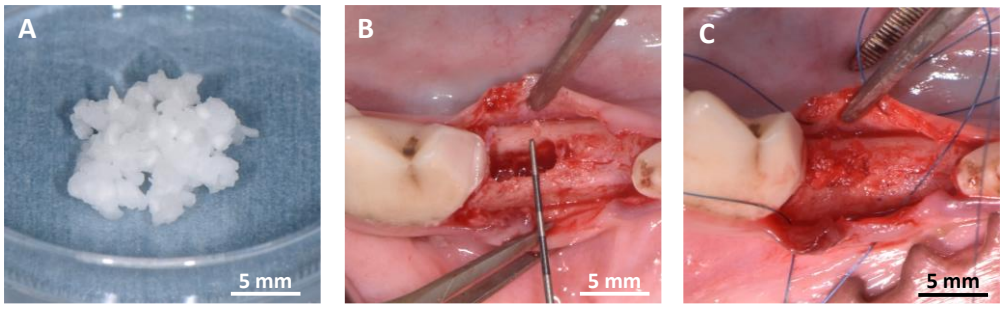

Figure 7. Surgical procedure of β-TCP/RCP granule implantation. (A) Digital photograph of β-TCP/RCP granules, (B) Surgically created 3-wall intrabony defect, (C) Placement of β-TCP/RCP into the defect. Abbreviations: RCP, recombinant human collagen peptide; TCP, tricalcium phosphate.

4.2 Implantation of β-TCP/RCP to experimental periodontal tissue defects

Five healthy 10-month-old female beagle dogs (Kitayama Labes Co. Ltd., Ina, Japan), weighing approximately 9 to 10 kg, were used in the experiments. Surgical procedures were performed under general anesthesia with intramuscular injection of midazolam (0.2 mg/kg body weight, Dormicum Injection 10 mg; Maruishi Pharmaceutical. Co., Ltd., Osaka, Japan), medetomidine hydrochloride (0.05 mg/kg body weight, Domitor; Nippon Zenyaku Kogyo Co., Ltd., Fukushima, Japan), butorphanol tartrate (0.2 mg/kg body weight, Vetorphale; Meiji Seika Pharma Co., Ltd., Tokyo, Japan). Lidocaine and adrenaline (Epilido cartridge; Nipro Corporation, Osaka, Japan) was used for local anesthesia in the surgical region.

Mandibular fourth premolars (both left and right side) of the beagle dogs were extracted, and an 8-week preoperative period was allowed for alveolar bone healing of the extraction socket. After healing, a mucoperiosteal flap was made and a three-walled infrabony defect (mesiodistal width × buccolingual width × depth: 5 mm × 3 mm × 4 mm) was created on the mesial side of the left and right mandibular first molar, using a dental carbide bar (GC Corporation, Tokyo, Japan) at 3000 rpm (Fig. 4B) [54]. The mesial surface of the mesial root of first molar was planed using a tooth planing bar (Dentech Corporation, Tokyo, Japan) to fully remove the alveolar bone and periodontal ligament tissue to be exposed in the bone defect. Subsequently, one defect was filled with 50 mg of β-TCP/RCP (designated as the β-TCP/RCP group, Fig. 4C) and the other defect was left empty (designated as the control group). The defects were completely covered with a mucoperiosteal flap with suturing. Ampicillin sodium (20 mg/kg, ampicillin sodium NZ for injection; Nippon Zenyaku Kogyo, Tokyo, Japan) was administered for 3 days after surgery. During the observation period, plaque control with 0.5% chlorhexidine (Hibiten; Dainippon Sumitomo Pharma, Tokyo, Japan) was performed twice weekly.

4.3 Micro-CT imaging and bone volume measurement

At 4 weeks (N=2) and 8 weeks (N=3) postoperatively, the dogs were euthanized with an overdose of sodium pentobarbital (SomnoPentyl; Kyoritsu Seiyaku Corporation, Tokyo, Japan) following general anesthesia and fixed via perfusion by 10% formalin (Mildform 10N, Fujifilm Wako Pure Chemical Corp.). The tissue blocks were removed, and the bone defects were imaged using a micro-CT (Latheta LCT-200; Hitachi, Ltd., Tokyo, Japan) to observe bone formation. In addition, the amount of new bone in 8-week specimens was quantified using imaging software (ImageJ; National Institutes of Health, Bethesda, MD, USA). After setting up a region of interest (ROI) of 5 mm x 4 mm (mesio-distal width x depth), the bone trabecular area was measured from a series of 30 bucco-lingual micro-CT images. The sum of the measurements was defined as the bone volume, and the percentage of the total volume of the ROI was calculated (BV/TV).

 doi:10.20944/preprints202210.0311.v1

4.4 Histological Observations

Tissue blocks were demineralized with 10% ethylenediaminetetraacetic acid and paraffin-embedded according to the conventional method. After slicing in the mesio-distal plane, sections were stained with HE, MT, and tartaric acid-resistant acid phosphatase (TRAP). In addition, specific antibodies were used to identify osteocalcin (OCN), CD3, CD204, and periostin (POSTIN). After the epitope retrieval step, sections were incubated overnight with primary antibodies: mouse anti-OCN (Takara Bio, Shiga, Japan), mouse anti-CD3 (Agilent Technologies Inc., Santa Clara, CA, USA), mouse anti-CD204 (Cosmo Bio Co., Ltd., Tokyo, Japan) and rabbit anti-POSTIN (Abcam plc., Cambridge, UK). The antigen-antibody reaction sites were visualized using diaminobenzidine. The stained sections were observed using an optical microscope (NanoZoomer S210; Hamamatsu Photonics K.K., Shizuoka, Japan).

4.5 Histometric measurements

Using MT-stained and POSTIN-stained images at 8 weeks after surgery and imaging software, the following properties were measured: (1) gingival tissue height (distance from the bottom of defect to the most coronally oriented point of the gingival tissue), (2) junctional epithelium height (distance from the bottom of defect to the most apical position of the junctional epithelium), (3) new bone height (distance from the bottom of defect to the most coronally oriented point of new bone-like tissue), (4) POSTIN expression tissue height (distance from the bottom of defect to the most coronally oriented point of the POSTIN-expressing tissue).

4.6 Statistical analysis

The values of micro-CT and histometric measurements of β-TCP/RCP and Ctrl groups were statistically analyzed using the two-tailed Mann-Whitney's U test. P-values of <0.05 were considered statistically significant. Statistical procedures were performed using the SPSS software package (version 11.0; IBM Corp., Armonk, NY, USA).

5. Conclusions

After β-TCP/RCP was implanted into experimental periodontal tissue defects, the effect of periodontal tissue healing was assessed in beagle dogs. Micro-CT analysis showed that the amount of new bone in the β-TCP/RCP group was significantly greater (2.2 fold) than in the Ctrl group at 8 weeks postoperatively. Histological findings showed the formation of bone-like and periodontal ligament-like tissue at the β-TCP/RCP implantation site. Histological measurements revealed that the periodontal tissue regeneration parameters in the β-TCP/RCP group were significantly greater than those in the Ctrl group. These results suggest that β-TCP/RCP is an effective material for promoting periodontal tissue regeneration.

Supplementary Materials: The following supporting information can be downloaded at: www.mdpi.com/xxx/s1, Supplemental Figure 1: HE stained sections.

Author Contributions: YY: methodology, validation, formal analysis, investigation, writing - original draft, visualization. HM: conceptualization, methodology, validation, formal analysis, investigation, writing - original draft, visualization, supervision. EN: validation, investigation. YK: investigation. AH: investigation. AK: validation, investigation, writing - review & editing. TS: resources, writing - review & editing. TA: investigation, writing - review & editing. All of the authors have approved the final version of the manuscript.

Funding: This research was supported by grants from the JSPS KAKENHI (Grant Nos. JP16K11822 and JP22K10012) and the 2020 AMED Translational Research Program (Grant No. A154).

Institutional Review Board Statement: Animal experiments were conducted in accordance with the institutional animal use and care regulations of Hokkaido University (Animal Research Committee of Hokkaido University, Approval number 19-84) and approved by the Animal Research

Committee of Hokkaido University. Experiments on animals were carried out in accordance with relevant guidelines and regulations.

Informed Consent Statement: Not applicable.
Data Availability Statement: The datasets are available from the corresponding author upon reasonable request.
Acknowledgments: This study was supported by Hokkaido University, which provided facilities and resources. β-TCP and RCP were kindly provided by Taihei Chemical Industrial Co., Ltd. and FUJIFILM Corp., respectively.

Conflicts of Interest: All authors have no conflicts of interest to disclose for this study.

References

1. Vaquette, C.; Pilipchuk, S.P.; Bartold, P.M.; Hutmacher, D.W.; Giannobile, W.V.; Ivanovski, S. Tissue engineered constructs for periodontal regeneration: current status and future perspectives. Adv. Healthc. Mater. 2018, 7, e1800457. doi: 10.1002/adhm.201800457.
2. Liu, Y.; Guo, L.; Li, X.; Liu, S.; Du, J.; Xu, J.; Hu, J.; Liu, Y. Challenges and tissue engineering strategies of periodontal-guided tissue regeneration. Tissue Eng. Part C Methods. 2022, 28, 405-419. doi: 10.1089/ten.TEC.2022.0106.
3. Iwata, T.; Yamato, M.; Tsuchioka, H.; Takagi, R.; Mukobata, S.; Washio, K.; Okano, T.; Ishikawa, I. Periodontal regeneration with multi-layered periodontal ligament-derived cell sheets in a canine model. Biomaterials. 2009, 30, 2716-2723. doi: 10.1016/j.biomaterials.2009.01.032.
4. Kawase, T.; Nagata, M.; Okuda, K.; Ushiki, T.; Fujimoto, Y.; Watanabe, M.; Ito, A.; Nakata, K. Platelet-rich fibrin extract: A promising fetal bovine serum alternative in explant cultures of human periosteal sheets for regenerative therapy. Int. J. Mol. Sci. 2019, 20, 1053. doi: 10.3390/ijms20051053.
5. Takedachi, M.; Sawada, K.; Sakura, K.; Morimoto, C.; Hirai, A.; Iwayama, T.; Shimomura, J.; Kawasaki K.; Fujihara, C.; Kashiwagi, Y.; Miyake, A.; Yamada, T.; Okura, H.; Matsuyama, A.; Saito, M.; Kitamura, M.; Murakami, S. Periodontal tissue regeneration by transplantation of autologous adipose tissue-derived multi-lineage progenitor cells. Sci. Rep. 2022, 12, 8126. doi: 10.1038/s41598-022-11986-z.
6. Anzai, J.; Nagayasu-Tanaka, T.; Terashima, A.; Asano, T.; Yamada, S.; Nozaki, T.; Kitamura, M.; Murakami, S. Long-term observation of regenerated periodontium induced by FGF-2 in the beagle dog 2-wall periodontal defect model. PLoS One. 2016, 11, e0158485. doi: 10.1371/journal.pone.0158485.
7. Shirakata, Y.; Nakamura, T.; Shinohara, Y.; Nakamura-Hasegawa, K.; Hashiguchi, C.; Takeuchi, N.; Imafuji, T.; Sculean, A.; Noguchi, K. Split-mouth evaluation of connective tissue graft with or without enamel matrix derivative for the treatment of isolated gingival recession defects in dogs. Clin. Oral Investig. 2019, 23, 3339-3349. doi: 10.1007/s00784-018-2750-1.
8. Ivanovski, S.; Vaquette, C.; Gronthos, S.; Hutmacher, D.W.; Bartold P.M. Multiphasic scaffolds for periodontal tissue engineering. J Dent Res. 2014, 93, 1212-1221. doi: 10.1177/0022034514544301.
9. Imber, JC.; Roccuzzo, A.; Stähli, A.; Saulacic, N.; Deschner, J.; Sculean, A.; Bosshardt D.D. Immunohistochemical evaluation of periodontal regeneration using a porous collagen scaffold. Int. J. Mol. Sci. 2021, 22, 10915. doi: 10.3390/ijms222010915.
10. Abdulghani, S.; Mitchell, G.R. Biomaterials for in situ tissue regeneration: A review. Biomolecules. 2019, 9, 750. doi: 10.3390/biom9110750.
11. Song, G.; Zheng, C.; Liu, Y.; Ding, M.; Liu, P.; Xu, J.; Wang, W.; Wang, J. In vitro extracellular matrix deposition by vascular smooth muscle cells grown in fibroin scaffolds, and the regulation of TGF-β1. Mater. Des. 2021, 199, 109428. doi: 10.1016/j.matdes.2020.109428.
12. Yoshida, T.; Miyaji, H.; Otani, K.; Inoue, K.; Nakane ,K.; Nishimura, H.; Ibara, A.; Shimada, A.; Ogawa, K.; Nishida, E.; Sugaya, T.; Sun, L.; Fugetsu, B.; Kawanami, M. Bone augmentation using a highly porous PLGA/β-TCP scaffold containing fibroblast growth factor-2. J. Periodont. Res. 2015, 50, 265-273. doi: 10.1111/jre.12206.
13. Ferreira, A.M.; Gentile, P.; Chiono, V.; Ciardelli, G. Collagen for bone tissue regeneration. Acta Biomater. 2012, 8, 3191-3200. doi: 10.1016/j.actbio.2012.06.014.
14. Kosen, Y.; Miyaji, H.; Kato, A.; Sugaya, T.; Kawanami, M. Application of collagen hydrogel/sponge scaffold facilitates periodontal wound healing in class II furcation defects in beagle dogs. J. Periodont. Res. 2012, 47, 626-634. doi: 10.1111/j.1600-0765.2012.01475.x.
15. Binlateh, T.; Thammanichanon, P.; Rittipakorn, P.; Thinsathid, N.; Jitprasertwong, P. Collagen-based biomaterials in periodontal regeneration: Current applications and future perspectives of plant-based collagen. Biomimetics (Basel). 2022, 7, 34. doi: 10.3390/biomimetics7020034.
16. Ramshaw, J.A. Biomedical applications of collagens. J. Biomed. Mater. Res. B Appl. Biomater. 2016, 104, 665-675. doi: 10.1002/jbm.b.33541.
17. Pawelec, K.M.; Confalonieri, D.; Ehlicke, F.; van Boxte,l H.A.; Walles, H.; Kluijtmans, S.G.J.M. Osteogenesis and mineralization of mesenchymal stem cells in collagen type I-based recombinant peptide scaffolds. J. Biomed. Mater. Res. A. 2017, 105, 1856-1866. doi: 10.1002/jbm.a.36049.

18. Parvizi, M.; Plantinga, J.A.; van Speuwel-Goossens, C.A.; van Dongen, E.M.; Kluijtmans, S.G.; Harmsen, M.C. Development of recombinant collagen-peptide-based vehicles for delivery of adipose-derived stromal cells. J. Biomed. Mater. Res. A. 2016, 104, 503-516. doi: 10.1002/jbm.a.35588.
19. Nakamura, K.; Iwazawa, R.; Yoshioka, Y. Introduction to a new cell transplantation platform via recombinant peptide petaloid pieces and its application to islet transplantation with mesenchymal stem cells. Transpl, Int. 2016, 29, 1039-1050. doi: 10.1111/tri.12810.
20. Akiyama, Y.; Ito, M.; Toriumi, T.; Hiratsuka, T.; Arai, Y.; Tanaka, S.; Futenma, T.; Akiyama, Y.; Yamaguchi, K.; Azuma, A.; Hata, K.I.; Natsume, N.; Honda, M. Bone formation potential of collagen type I-based recombinant peptide particles in rat calvaria defects. Regen. Ther. 2020, 16, 12-22. doi: 10.1016/j.reth.2020.12.001.
21. Miyamoto, M.; Nakamura, K.; Shichinohe, H.; Yamauchi, T.; Ito, M.; Saito, H.; Kawabori, M.; Osanai, T.; Sasaki, T.; Houkin, K.; Kuroda, S. Human recombinant peptide sponge enables novel.; Less invasive cell therapy for ischemic stroke. Stem Cells Int. 2018, 2018, 4829534. doi: 10.1155/2018/4829534.
22. Mashiko, T.; Takada, H.; Wu, S.H.; Kanayama, K.; Feng, J.; Tashiro, K.; Asahi, R.; Sunaga, A.; Hoshi, K.; Kurisaki, A.; Takato, T.; Yoshimura, K. Therapeutic effects of a recombinant human collagen peptide bioscaffold with human adipose-derived stem cells on impaired wound healing after radiotherapy. J. Tissue Eng. Regen. Med. 2018, 12, 1186-1194. doi: 10.1002/term.2647.
23. Zhang, D.; Wu, X.; Chen, J.; Lin, K. The development of collagen based composite scaffolds for bone regeneration. Bioact. Mater. 2017, 3, 129-138. doi: 10.1016/j.bioactmat.2017.08.004.
24. Murakami, S.; Miyaji, H.; Nishida, E.; Kawamoto, K.; Miyata, S.; Takita, H.; Akasaka, T.; Fugetsu, B.; Iwanaga, T.; Hongo, H.; Amizuka, N.; Sugaya, T.; Kawanami, M. Dose effects of beta-tricalcium phosphate nanoparticles on biocompatibility and bone conductive ability of three-dimensional collagen scaffolds. Dent. Mater. J. 2017, 36, 573-583. doi: 10.4012/dmj.2016-295.
25. Ogawa, K.; Miyaji, H.; Kato, A.; Kosen, Y.; Momose, T.; Yoshida, T.; Nishida, E.; Miyata, S.; Murakami, S.; Takita, H.; Fugetsu, B.; Sugaya, T.; Kawanami, M. Periodontal tissue engineering by nano beta-tricalcium phosphate scaffold and fibroblast growth factor-2 in one-wall infrabony defects of dogs. J. Periodont. Res. 2016, 51, 758-767. doi: 10.1111/jre.12352.
26. Oshima, S.; Sato, T.; Honda, M.; Suetsugu, Y.; Ozeki, K.; Kikuchi, M. Fabrication of gentamicin-loaded hydroxyapatite/collagen bone-like nanocomposite for anti-infection bone void fillers. Int. J. Mol. Sci. 2020, 21, 551. doi: 10.3390/ijms21020551.
27. Kawai, T.; Echigo, S.; Matsui, K.; Tanuma, Y.; Takahashi, T.; Suzuki, O.; Kamakura, S. First clinical application of octacalcium phosphate collagen composite in human bone defect. Tissue Eng. Part A. 2014, 20, 1336-1341. doi: 10.1089/ten.TEA.2013.0508.
28. Santhakumar, S.; Oyane, A.; Nakamura, M.; Yoshino, Y.; Alruwaili, MK.; Miyaji, H. Bone tissue regeneration by collagen scaffolds with different calcium phosphate coatings: amorphous calcium phosphate and low-crystalline apatite. Materials (Basel). 2021, 14, 5860. doi: 10.3390/ma14195860.
29. Kanemoto, Y.; Miyaji, H.; Nishida, E.; Miyata, S.; Mayumi, K.; Yoshino, Y.; Kato, A.; Sugaya, T.; Akasaka, T.; Nathanael, A.J.; Santhakumar, S.; Oyane, A. Periodontal tissue engineering using an apatite/collagen scaffold obtained by a plasma- and precursor-assisted biomimetic process. J Periodont. Res. 2022, 57, 205-218. doi: 10.1111/jre.12954.
30. Furihata, T.; Miyaji, H.; Nishida, E.; Kato, A.; Miyata, S.; Shitomi, K.; Mayumi, K.; Kanemoto, Y.; Sugaya, T.; Akasaka, T. Bone forming ability of recombinant human collagen peptide granules applied with β-tricalcium phosphate fine particles. J. Biomed. Mater. Res. B Appl. Biomater. 2020, 108, 3033-3044. doi: 10.1002/jbm.b.34632.
31. Tamura, Y.; Takeuchi, Y.; Suzawa, M.; Fukumoto, S.; Kato, M.; Miyazono, K.; Fujita, T. Focal adhesion kinase activity is required for bone morphogenetic protein—Smad1 signaling and osteoblastic differentiation in murine MC3T3-E1 cells. J. Bone Miner. Res. 2001, 16, 1772-1779. doi: 10.1359/jbmr.2001.16.10.1772.
32. Jeong, J.; Kim, J.H.; Shim, J.H.; Hwang, N.S.; Heo, C.Y. Bioactive calcium phosphate materials and applications in bone regeneration. Biomater. Res. 2019, 23, 4. doi: 10.1186/s40824-018-0149-3.
33. Maazouz, Y.; Rentsch, I.; Lu, B.; Santoni, B.L.G.; Doebelin, N.; Bohner, M. In vitro measurement of the chemical changes occurring within β-tricalcium phosphate bone graft substitutes. Acta Biomater. 2020, 102, 440-457. doi: 10.1016/j.actbio.2019.11.035.
34. Chang, Y.L.; Stanford, C.M.; Keller, J.C. Calcium and phosphate supplementation promotes bone cell mineralization: implications for hydroxyapatite (HA)-enhanced bone formation. J. Biomed. Mater. Res. 2000, 52, 270-278. doi: 10.1002/1097-4636(200011)52:2<270::aid-jbm5>3.0.co;2-1.
35. Dvorak, M.M.; Siddiqua, A.; Ward, D.T.; Carter, D.H.; Dallas, S.L.; Nemeth, E.F.; Riccardi, D. Physiological changes in extracellular calcium concentration directly control osteoblast function in the absence of calciotropic hormones. Proc. Natl. Acad. Sci. U. S. A. 2004, 101, 5140-5145. doi: 10.1073/pnas.0306141101.
36. Kanatani, M.; Sugimoto, T.; Kano, J.; Kanzawa, M.; Chihara, K. Effect of high phosphate concentration on osteoclast differentiation as well as bone-resorbing activity. J. Cell Physiol. 2003, 196, 180-189. doi: 10.1002/jcp.10270.
37. Sheikh, Z.; Qureshi, J.; Alshahrani, A.M.; Nassar, H.; Ikeda, Y.; Glogauer, M.; Ganss, B. Collagen based barrier membranes for periodontal guided bone regeneration applications. Odontology. 2017, 105, 1-12. doi: 10.1007/s10266-016-0267-0.
38. Muraya, K.; Kawasaki, T.; Yamamoto, T.; Akutsu, H. Enhancement of cellular adhesion and proliferation in human mesenchymal stromal cells by the direct addition of recombinant collagen I peptide to the culture medium. Biores. Open Access. 2019, 8, 210-218. doi: 10.1089/biores.2019.0012.
39. Naritomi, M.; Mizuno, M.; Katano, H.; Ozeki, N.; Otabe, K.; Komori, K.; Fujii, S.; Ichinose, S.; Tsuji, K.; Koga, H.; Muneta, T.; Sekiya, I. Petaloid recombinant peptide enhances in vitro cartilage formation by synovial mesenchymal stem cells. J. Orthop. Res. 2019, 37, 1350-1357. doi: 10.1002/jor.24042.
40. Gothard, D.; Smith, E.L.; Kanczler, J.M.; Black, C.R.; Wells, J.A.; Roberts, C.A.; White, L.J.; Qutachi, O.; Peto, H.; Rashidi, H.; Rojo, L.; Stevens, M.M.; El Haj, A.J.; Rose, F.R.; Shakesheff, K.M.; Oreffo, R.O. In vivo assessment of bone regeneration in

alginate/bone ECM hydrogels with incorporated skeletal stem cells and single growth factors. PLoS One. 2015, 10, e0145080. doi: 10.1371/journal.pone.0145080.

41. Lin, H.; Tang, Y.; Lozito, T.P.; Oyster, N.; Wang, B.; Tuan, R.S. Efficient in vivo bone formation by BMP-2 engineered human mesenchymal stem cells encapsulated in a projection stereolithographically fabricated hydrogel scaffold. Stem Cell Res. Ther. 2019, 10, 254. doi: 10.1186/s13287-019-1350-6.
42. Bousnaki, M.; Beketova, A.; Kontonasaki, E. A review of in vivo and clinical studies applying scaffolds and cell sheet technology for periodontal ligament regeneration. Biomolecules. 2022, 12, 435. doi: 10.3390/biom12030435.
43. Takahashi, D.; Odajima, T.; Morita, M.; Kawanami, M.; Kato, H. Formation and resolution of ankylosis under application of recombinant human bone morphogenetic protein-2 (rhBMP-2) to class III furcation defects in cats. J. Periodont. Res. 2005, 40, 299-305. doi: 10.1111/j.1600-0765.2005.00794.x.
44. Horiuchi, K.; Amizuka, N.; Takeshita, S.; Takamatsu, H.; Katsuura, M.; Ozawa, H.; Toyama, Y.; Bonewald, L.F.; Kudo, A. Identification and characterization of a novel protein.; periostin.; with restricted expression to periosteum and periodontal ligament and increased expression by transforming growth factor beta. J. Bone Miner. Res. 1999, 14, 1239-1249. doi: 10.1359/jbmr.1999.14.7.1239.
45. Du, J.; Li, M. Functions of periostin in dental tissues and its role in periodontal tissues' regeneration. Cell Mol. Life Sci. 2017, 74, 4279-4286. doi: 10.1007/s00018-017-2645-3.
46. Park, C.H.; Rios, H.F.; Jin, Q.; Sugai, J.V.; Padial-Molina, M.; Taut, A.D.; Flanagan, C.L.; Hollister, SJ.; Giannobile, W.V. Tissue engineering bone-ligament complexes using fiber-guiding scaffolds. Biomaterials. 2012, 33, 137-145. doi: 10.1016/j.biomaterials.2011.09.057.
47. Pilipchuk, S.P.; Fretwurst, T.; Yu, N.; Larsson, L.; Kavanagh, N.M.; Asa'ad, F.; Cheng, K.C.K.; Lahann, J.; Giannobile, W.V. Micropatterned scaffolds with Immobilized growth factor genes regenerate bone and periodontal ligament-like tissues. Adv. Healthc. Mater. 2018, 7, e1800750. doi: 10.1002/adhm.201800750.
48. Basu, A.; Rothermund, K.; Ahmed, M.N.; Syed-Picard, F.N. Self-assembly of an organized cementum-periodontal ligament-like complex using scaffold-free tissue engineering. Front Physiol. 2019, 10, 422. doi: 10.3389/fphys.2019.00422.
49. Arzate, H.; Zeichner-David, M.; Mercado-Celis, G. Cementum proteins: role in cementogenesis.; biomineralization.; periodontium formation and regeneration. Periodontol 2000. 2015, 67, 211-233. doi: 10.1111/prd.12062.
50. Arweiler, N.B.; Netuschil, L. The oral microbiota. Adv. Exp. Med. Biol. 2016, 902, 45-60. doi: 10.1007/978-3-319-31248-4_4.
51. Katagiri, H.; Mendes, L.F.; Luyten, FP. Reduction of BMP6-induced bone formation by calcium phosphate in wild-type compared with nude mice. J. Tissue Eng. Regen. Med. 2019, 13, 846-856. doi: 10.1002/term.2837.
52. Kurashina, K.; Kurita, H.; Wu, Q.; Ohtsuka, A.; Kobayashi, H. Ectopic osteogenesis with biphasic ceramics of hydroxyapatite and tricalcium phosphate in rabbits. Biomaterials. 2002, 23, 407-412. doi: 10.1016/s0142-9612(01)00119-3.
53. Kamakura, S.; Sasano, Y.; Shimizu, T.; Hatori, K.; Suzuki, O.; Kagayama, M.; Motegi, K. Implanted octacalcium phosphate is more resorbable than beta-tricalcium phosphate and hydroxyapatite. J. Biomed. Mater. Res. 2002, 59, 29-34. doi: 10.1002/jbm.1213.
54. Nagayasu-Tanaka, T.; Anzai, J.; Takaki, S.; Shiraishi, N.; Terashima, A.; Asano, T.; Nozaki, T.; Kitamura, M.; Murakami, S. Action mechanism of fibroblast growth factor-2 (FGF-2) in the promotion of periodontal regeneration in beagle dogs. PLoS One. 2015, 10, e0131870. doi: 10.1371/journal.pone.0131870.